HHS Public Access

Author manuscript

Hippocampus. Author manuscript; available in PMC 2017 April 01.

Published in final edited form as:

Hippocampus. 2016 April ; 26(4): 455–471. doi:10.1002/hipo.22535.

Deficits in hippocampal-dependent transfer generalization learning accompany synaptic dysfunction in a mouse model of amyloidosis

Karienn S. Montgomery[1], **George Edwards III**[2], **Yona Levites**[3], **Ashok Kumar**[3], **Catherine E. Myers**[4,5], **Mark A. Gluck**[6], **Barry Setlow**[7], and **Jennifer L. Bizon**[3]

[1]Department of Neuroscience and Experimental Therapeutics, Texas A&M Health Science Center, Bryan, TX

[2]Mitchell Center for Alzheimer's Disease and Related Brain Disorders, Department of Neurology, University of Texas Health Science Center in Houston, Houston, TX

[3]Department of Neuroscience, University of Florida, Gainesville, FL

[4]VA New Jersey Health Care System, East Orange, NJ 07018

[5]Department of Pharmacology, Physiology & Neuroscience, New Jersey Medical School, Rutgers University, Newark, NJ

[6]Center for Molecular & Behavioral Neuroscience, Rutgers University, Newark, NJ

[7]Department of Psychiatry, University of Florida, Gainesville, FL

Abstract

Elevated β-amyloid and impaired synaptic function in hippocampus are among the earliest manifestations of Alzheimer's disease (AD). Most cognitive assessments employed in both humans and animal models, however, are insensitive to this early disease pathology. One critical aspect of hippocampal function is its role in episodic memory, which involves the binding of temporally coincident sensory information (e.g., sights, smells, and sounds) to create a representation of a specific learning epoch. Flexible associations can be formed among these distinct sensory stimuli that enable the "transfer" of new learning across a wide variety of contexts. The current studies employed a mouse analog of an associative "transfer learning" task that has previously been used to identify risk for prodromal AD in humans. The rodent version of the task assesses the transfer of learning about stimulus features relevant to a food reward across a series of compound discrimination problems. The relevant feature that predicts the food reward is unchanged across problems, but an irrelevant feature (i.e., the context) is altered. Experiment 1 demonstrated that C57BL6/J mice with bilateral ibotenic acid lesions of hippocampus were able to discriminate between two stimuli on par with control mice; however, lesioned mice were unable to transfer or apply this learning to new problem configurations. Experiment 2 used the $APP_{swe}PS1$ mouse model of amyloidosis to show that robust impairments in transfer learning are evident in

Address Correspondence to: Jennifer L. Bizon, Ph.D., Department of Neuroscience, McKnight Brain Institute, University of Florida, Gainesville, FL 32610-0244, P.O. Box 100244, Office: 352-294-5149, bizonj@ufl.edu.

None of the authors declare any conflicts of interest.

mice with subtle β amyloid-induced synaptic deficits in the hippocampus. Finally, Experiment 3 confirmed that the same transfer learning impairments observed in $APP_{swe}PS1$ mice were also evident in the Tg-SwDI mouse, a second model of amyloidosis. Together, these data show that the ability to generalize learned associations to new contexts is disrupted even in the presence of subtle hippocampal dysfunction and suggest that, across species, this aspect of hippocampal-dependent learning may be useful for early identification of AD-like pathology.

Keywords

associative learning; synaptic function; LTP; memory; amyloid; APPswePS1; Tg-SwDI; Alzheimer's disease; mice

INTRODUCTION

Molecular and functional changes in the hippocampus are among the earliest to manifest in Alzheimer's disease [AD (Dubois et al., 2007; Ferreira et al., 2011; Lowndes et al., 2008)]. Many of the cognitive assessments used to diagnose AD are thus designed to evaluate hippocampal function, with a particular focus on declarative memory (e.g., delayed paragraph recall (Gluck et al., 2006; Moodley et al., 2015; Silva et al., 2012)). Despite such tasks demonstrating high reliability for classifying individuals with moderate AD, these assessments are suboptimal in their early diagnostic utility (Maruff et al., 2004). Indeed, the vast majority of individuals who demonstrate impaired performance on declarative memory tasks already have pronounced, multifaceted forms of hippocampal pathology and neurodegeneration (Jack et al., 2011; Kluger et al., 1999). The ability to detect individuals in prodromal stages of AD would offer a unique therapeutic window for prolonging the duration of good cognitive functioning and slowing disease progression (Rabin et al., 2012).

During new memory formation, the hippocampus forms connections between sensory stimuli that are experienced together (Gluck and Myers, 1993; Gluck and Myers, 1995; Johnson et al., 2008). Such temporally precise encoding of information from multiple sensory modalities forms the basis of "episodic memory" (Eichenbaum and Cohen, 2014; McKenzie et al., 2014). In addition, the hippocampal region is critical for the development of appropriate representations of newly learned associations, such as in classical or operant conditioning, allowing the past learning to generalize to novel situations or contexts, an ability that is important for adaptive behavior (Myers and Gluck, 1996). Evidence that the hippocampus supports such generalization is found in animal studies in which rats and nonhuman primates with hippocampal damage "unitize" stimuli (or stimulus features) during learning, resulting in impairments when aspects of the learned stimuli are altered and presented in novel combinations or contexts (Barense et al., 2005; Eichenbaum et al., 1988; Eichenbaum et al., 1987; Etchamendy, 2003; Quamme et al., 2007; Rudy and Sutherland, 1995).

Based on such animal studies, Myers, Gluck and colleagues developed a novel computer-based associative learning task to assess hippocampal function in humans (Myers et al., 2002). The task, which is described in detail in Myers et al. (2002), involves a series of two-object visual discrimination problems in which subjects learn by trial-and-error to choose

the correct object within each pair. The objects have two stimulus features (shape and color). Within each pair, objects differ with respect to either their color or shape (the "relevant" feature), but not both. The other feature is common across both objects in a given pair and is thus irrelevant to the correct choice. After learning a series of these discrimination problems to criterion, a reconfigured series of problems is presented in which the irrelevant feature of each object pair is changed but the relevant feature remains the same and still predicts the correct choice. On these new problems, subjects must "transfer" their original learning about the correct object in each pair to the new context that contains the novel, but irrelevant feature. Aged subjects with mild hippocampal atrophy and increased risk for AD are able to learn the initial discrimination problems on par with control subjects. These individuals are significantly impaired, however, when required to "transfer" the previously-learned associations to the new, reconfigured problems, despite the fact that the stimulus feature predictive of the correct choice does not change (Myers et al., 2002). The relationship between transfer learning deficits and hippocampal atrophy suggests that the behavioral deficits are mediated by the hippocampus and that assays that probe this aspect of hippocampal function may be particularly sensitive to subtle changes in hippocampal integrity (Krishna et al., 2012; Myers et al., 2008a; Myers et al., 2002; Myers et al., 2008b).

In addition to potentially having advantages for early detection of disease pathology, "transfer learning" tasks may have a secondary advantage within AD research. Specifically, as these task designs are grounded in findings from animal studies, it should be possible to develop highly analogous, species-specific versions of transfer learning tasks that could facilitate translation between human subjects and animal models of aging and age-related disease. Indeed, prior work from our laboratory established a transfer learning task that is readily learned by mice (Montgomery et al., 2011). Using this task, 12 month old $APP_{swe}PS1$ transgenic mice with advanced amyloidosis (Jankowsky et al., 2004) showed behavioral deficits that mirrored those in aged humans with hippocampal atrophy. Notably, however, in this previous study, behavioral deficits were not explicitly linked to hippocampal integrity. In the current study, ibotenic acid lesions were used to determine whether transfer learning performance critically depends on the hippocampal formation. Experiments were then conducted to both characterize synaptic dysfunction in the $APP_{swe}PS1$ mouse model at earlier ages than typically studied (i.e., 6 months) and to assess whether such dysfunction is sufficient to produce reliable transfer learning deficits. Finally, experiments were designed to test whether the transfer learning deficits in $APP_{swe}PS1$ mice generalized to a second mouse model of amyloidosis (Tg-SwDI mice).

MATERIALS & METHODS

Experiment 1: Dependence of transfer generalization learning on hippocampus

Subjects—Female C57BL6/J mice (n=14, obtained from The Jackson Laboratory) were housed in the AAALAC-accredited vivarium in the Department of Psychology at Texas A&M University. Upon arrival, mice were given at least two weeks with *ad libitum* access to food and water to habituate to vivarium conditions prior to surgery. Mice were maintained on a 12-h light/dark cycle (lights on at 0800). All experiments took place during the light phase of the cycle and were conducted in accordance with approved institutional animal care

procedures and NIH guidelines. One week prior to behavioral testing, mice were food-restricted to 85% of their free-feeding weight and handled for 3-5 minutes daily to habituate to the experimenter. During this time, mice were individually housed in order to maintain strict control over food consumption. Upon completion of behavioral testing, mice were returned to *ad libitum* food.

Hippocampal Lesion Procedures—Mice were anesthetized with isoflurane and placed in a stereotaxic apparatus (Kopf Instruments, Tujunga, California, USA) fitted with a gas anesthesia system. A midline incision was made and holes were drilled in the skull over the lesion sites. A 30-gauge needle attached to a 10 μl microsyringe (Hamilton, Reno, NV, USA) mounted on a timer-controlled infusion pump (Sage Instruments, Boston, MA, USA) was used for injections. Ibotenic acid (Sigma, St Louis, MO, USA) was dissolved in phosphate-buffered saline (PBS; final pH of 7.4) at a concentration of 10 μg/μl. A volume of 0.05 μl was injected at each of four sites per hemisphere at the following coordinates (in mm, AP, ML, DV relative to bregma and the skull surface at the drill site): −1.7, ±1.3, −1.9; −2.1, ±2.8, −3.0; −2.4, ±2.9, −4.0; −2.8, ±3.1, −3.7 (Desmedt et al., 2003; Franklin and Paxinos, 2008). Sham-operated mice underwent the same procedure except that PBS alone was injected. The incision was closed with wound clips, and mice were monitored until recovery from anesthesia. Mice were given a two week recovery period prior to the start of behavioral testing.

Behavioral Testing

Apparatus: The testing apparatus and procedures for the transfer learning task are described in detail in Montgomery et al. (2011). Briefly, the apparatus consisted of an open-topped black Plexiglas box (30 cm width; 45 cm length; 20 cm deep) with two small terra cotta flower pots (4 cm diameter; 3 cm deep) secured to the floor with velcro at one end of the box. Twenty mg chocolate-flavored food pellets (AIN-76A, TestDiet) were used as the reward in the task.

Shaping Procedures: Testing began with a shaping procedure designed to train the mice to dig in the pots to obtain the food rewards. On each trial, mice were placed at the end of the box distal from the pots, and were required to approach the pots to retrieve the food rewards. Initially, a food reward was placed in each of the (empty) pots, and the trial ended when mice consumed the reward from each pot. After 12 trials of successively retrieving both pellets from the empty pots, the pots were filled with progressively greater volumes of a mixture of the various digging media (e.g., beads, yarn, wood shavings) used for the task (12 trials each at 33%, 50% and 100% filled), such that the mice learned to dig through the media in order to obtain the food rewards.

On the day after successfully retrieving both pellets from completely filled pots, mice were given a single “shaping” discrimination problem (odor or media, counterbalanced across groups) in order to train them in the procedural aspects of the task. During discrimination problems, only one of the pots contained the food reward, and crushed food pellets were sprinkled over the surface of both pots to disguise the odor of the food (i.e., to make it more difficult to detect the location of the food on the basis of its odor). The left/right position of

the rewarded pot varied pseudo-randomly across trials. For the first four trials of each discrimination problem, mice were allowed to dig in both pots until they obtained the reward (i.e. they were allowed to self-correct if they dug initially in the incorrect pot). On these trials, only their first choice was scored as correct or incorrect. On trials thereafter, mice were removed from the test chamber after only one dig (either correct or incorrect). A dig in a pot was scored if a mouse displaced the digging media with either its paws or nose.

For discrimination problems, mice learned to discriminate between the pots with two stimulus features (either distinct odorants applied to the rims of the pots or distinct digging media filling the pots). One of the two pots was paired with a food reward, with either the odor or the digging media used as the "relevant" feature. For half the discrimination problems, odor was the relevant feature, and thus the pots differed in odor (with one odor always predictive of the food reward; e.g., rose+ versus citrus−) but contained the same digging media (e.g., beads) that was thus irrelevant to the correct choice. For the other half of the discrimination problems, the digging medium was the relevant feature that differed between pots and predicted the reward (e.g., yarn+ versus wood shavings−), and the pots were scented with the same odor (e.g., vanilla) that was irrelevant to the correct choice.

Transfer Learning Task Procedures: As with the human transfer learning task (Myers et al., 2002), testing in the mouse task was conducted in a single session. Initially, mice were trained on a series of three concurrent discrimination problems (the "learning phase" of the task). New discrimination problems were introduced progressively, intermixed with already-learned pairs as criterion performance was reached on each problem set. Criterion performance was defined as 6 consecutive correct choices. The rewarded and unrewarded stimuli in each discrimination pair and the sequence of discrimination problems were randomized across mice, although each mouse received discrimination problems in which the relevant feature alternated between odor and digging media. The learning phase began with two distinct discrimination problems presented in pseudo-random order (Problem Set 1). Once criterion performance was reached on these problems (6 consecutive correct choices, including 3 from each problem), a third problem was introduced and the three pairs of media/odor combinations were presented in a pseudorandom order (Problem Set 2) until mice again reached criterion performance (6 consecutive correct choices, including 2 from each problem). This design ensured that each discrimination pair was learned prior to the transfer phase. The number of trials required to reach criterion was used as the measure of performance.

After reaching criterion performance, mice were immediately assessed in the transfer phase of the task. During the transfer phase, mice were presented with 30 trials on which only the irrelevant stimulus feature in each discrimination problem was changed, and the 3 new combinations were intermixed (including 10 each of the three discriminations). This design allowed for assessment of the ability to transfer the predictive value of the previously-learned relevant feature (e.g., a particular odor) to a new context (e.g., pots containing a novel digging medium). The percentage of incorrect choices (errors) was used as the measure of performance.

Odor Detection Threshold Testing: Both hippocampal damage and amyloidosis have been associated with altered olfactory function (Kesner et al., 2011; Thompson et al., 1998; Velayudhan L et al., 2015; Weeden et al., 2014). As olfactory abilities are integral to performance on the transfer learning task, mice were assessed for their ability to detect decreasing dilutions of an odorant. Following completion of the transfer learning task, mice were trained to criterion on one additional odor discrimination problem (a full strength odorant which was always rewarded vs. virtually odorless mineral oil). Both pots were filled with mixed digging media. Once achieving criterion performance on this problem (6 consecutive correct trials), mice were tested on the same discrimination problem in which the full strength odorant was systematically diluted (1/100, 1/1000, 1/10000, 1/100000 for mice in Experiment 1; 1/100, 1/1000, 1/10000 for mice in Experiment 2). Mice were given 16 trials at each dilution and the percentage of incorrect trials was used as the measure of performance.

Histological Assessment of Hippocampal Lesions—Following completion of behavioral testing, mice were administered a lethal dose of pentobarbital and perfused intracardially with 0.9% saline followed by 4% paraformaldehyde. Brains were extracted and stored in 4% paraformaldehyde for 24 h, after which they were placed in a 30% sucrose/PBS solution for 24 hours. Brains were then frozen and sectioned (30 μm) coronally through the entire hippocampus on a calibrated freezing microtome. Sections were mounted on gelatin-coated glass slides, stained with thionin (0.25%), dehydrated in ascending concentrations of ethanol, delipidated in xylene, and coverslipped with Permount (Cahill et al., 2000). For lesion verification, sections were visualized on a Zeiss AxioImager. M2 microscope. The perimeter of tissue damage was outlined with the assistance of Stereo Investigator software (MBF Biosciences, Williston, VT). Tracings were compared to plates from a mouse brain atlas corresponding to the rostro-caudal extent of hippocampus (Franklin and Paxinos, 2008). Percent loss of hippocampal volume was determined using the ruler tool in Aperio ImageScope software. In each section, a tracing of spared hippocampus was compared to a tracing of the entire area of the hippocampal region. All mice presented less than 5% sparing of the hippocampal region bilaterally, and hence none were excluded from subsequent analyses.

Statistical Analyses—The number of trials required for criterion performance at each phase of task acquisition and initial discrimination learning (shaping problem, Problem Set 1, Problem Set 2) was compared between experimental groups using unpaired t-tests. For the transfer phase, on which a fixed number of trials (30) was presented, the percentage of those trials on which an incorrect choice was made (errors) was compared between groups using an unpaired t-test. For odor detection threshold testing, an unpaired t-test was used to compare trials to criterion on discrimination of the full strength odorant versus no odorant. A two-factor repeated-measures ANOVA (lesion condition × odor dilution) was then used to compare performance (percent error at each dilution) across the progressive dilutions of the full-strength odorant. Statistical comparisons were conducted in SPSS 22.0, and p values less than 0.05 were considered significant.

Experiment 2: Synaptic dysfunction and transfer learning performance in the APPswePS1 model of amyloidosis

Subjects—Breeder pairs were acquired from The Jackson Laboratory and bred in the University of Florida's Department of Animal Care Services (ACS), an AAALAC approved barrier facility. A cohort was formed by hemizygous crossing between B6C3F1/J and B6C3-Tg(APPswe,PSEN1dE9)85Dbo/J) mice. F1 offspring from hemizygous $APP_{swe}PS1$ breeders were genotyped at 2 months of age, and female $APP_{swe}PS1$ and non-transgenic littermate control (NTg) mice were transferred to the AAALAC-accredited vivarium in the McKnight Brain Institute (University of Florida College of Medicine), where they were individually housed and allowed to habituate to vivarium conditions with *ad libitum* access to food and water for at least one month prior to the start of experiments. Mice used in the transfer learning task were food-restricted to 85% of their free-feeding weight for one week prior to behavioral testing and handled for 3-5 minutes daily to habituate to the experimenter. Upon completion of behavioral testing, these mice were returned to *ad libitum* food. As behavioral testing can alter synaptic function in mouse models of amyloidosis (Jankowsky et al., 2003; Lazarov et al., 2005; Mainardi et al., 2014; Montarolo et al., 2013; Stargardt et al., 2015), mice used for biochemical and electrophysiological experiments were not behaviorally tested.

Tissue Harvesting and Aβ Assessment—Behaviorally naïve NTg (6 mo., n=4) and $APP_{swe}PS1$ (3 mo., n=5 and 6 mo., n=7) mice were sacrificed for Aβ assessment. Mice were perfused with 0.1 M PBS, and brains were removed from the cranium and hemisected along the midline. The hippocampus was dissected from one hemisphere, frozen in liquid nitrogen, and stored at −80°C until Aβ analysis with Enzyme-Linked Immunosorbent Assay (ELISA). The remaining intact hemisphere was prepared for histological analysis of plaque deposition by Thioflavin-S staining. Hemi-brains were immersion-fixed (at 4°) for 48 h in 4% paraformaldehyde in 0.1 M phosphate buffer (PBS, pH 7.4), cryoprotected in 20% sucrose in 0.1 M PBS for 48 h, rapidly frozen on powdered dry ice, and stored at −80°C until processing.

Enzyme-linked immunosorbent assay (ELISA): Homogenates were prepared from the dissected hippocampi in order to quantify Aβ40 and 42 levels using ELISA. Tissue was first homogenized using a tissue homogenizer in radioimmunoprecipitation assay (RIPA) buffer (50 mM Tris-HCl pH 7.4, 150 mM NaCl, 1% NP-40, 1% sodium deocycholate, 0.5% SDS) in the presence of protease inhibitor (10 μl/mL) and 0.5 M ethylenediaminetetraacetic acid (EDTA). Samples were sonicated and centrifuged at 13,000g for 20 minutes at 4°. Protein concentration was determined using the Pierce BCA Kit according to the manufacturer's protocol (Rockford, IL, USA), using an iMARK Microplate Absorbance Reader (BioRad) to detect protein concentrations at λ550 nm. One aliquot of the resultant supernatant was collected and stored at −80° for subsequent immunoblotting assays. To obtain the RIPA-soluble fraction for ELISA analysis, supernatant was collected from a second aliquot following further vacuum-centrifugation at 100,000 g for one hour at 4°. Following centrifugation, the resultant supernatant (SDS-soluble fraction) was collected. The resultant pellet was then extracted in 70% formic acid (FA), centrifuged, and the supernatant collected (FA fraction).

Sandwich capture ELISA was used with mAb9 capture and mAb40.1-HRP detection for Aβ40 and mAb42.2 capture and mAb9-HRP detection for Aβ42. These antibodies were developed in the laboratory of Dr. Todd Golde and have been extensively characterized in previous publications (Levites et al., 2006a; Levites et al., 2006b). Immunolon HBX4 plates were coated with 100 μL of 25 μg/mL antibody in PBS per well and stored at 4° overnight. Antibodies were then removed from plates and blocked with accessory reagent (1% Block ACE, 0.05% NaN3, 10X PBS, pH 7.4) at 4° overnight. RIPA homogenate aliquots were further diluted 1:5 for Aβ 1-42 and 1:10 for Aβ 1-40. After ACE blocking was removed, wells were washed with 300 μL of PBS, and 50 EC buffer (antigen capture buffer; NaH_2PO_4, NaN_3, EDTA, NaCl, BSA, CHAPS lysis buffer, pH 7.0) was added to the plate, and 100 μL of sample was added to duplicate wells. The plate was then incubated overnight at 4°. Fluid was discarded from the plate, and wells were washed with 300 μL of PBS. Antibodies were added at 1:1000 concentration (diluted in detection buffer; NaH2PO4, Na3PO4, thimerosal, EDTA, NaCl, bovine serum albumin (BSA) at pH 7.0) and incubated overnight at 4°. Plates were washed with PBST and PBS, and TMB (developing solution; 1 M Tris Base, 0.5 M Na2HPO4, peroxide) was added to each well. Stopping buffer (85% phosphoric acid) was added when optimal development was achieved (i.e., color was achieved in at least 3 standards). Detection was performed at λ 450nm and stored at 4°. All values were calculated as picomoles per gram (pm/g) based on the initial weight of brain tissue. Aβ40 and Aβ42 values were compared between groups using one-factor ANOVA.

Thioflavin-S staining procedures and plaque quantification: Aβ plaques were evaluated in the intact hemispheres of the brains used for ELISA analysis. Cryoprotected hemi-brains were sectioned at 30 μm in the coronal plane through the hippocampus using a calibrated freezing microtome. Sections through dorsal hippocampus (1 in 6 series) were collected into 0.1 M tris-buffered saline (TBS), and then mounted onto gelatin-coated glass slides. For staining, slides were rehydrated in running water and sequentially incubated in $KMnO_4$ (0.25%), $K_2S_2O_5$ /Oxalic Acid (1%), and Thioflavin-S (Sigma, 0.02%). Staining was differentiated using ethanol (80%). Slides were coverslipped with Prolong Gold, sealed, and stored in the dark at 4° until analysis. For analysis of plaque burden, n=6 sections/animal, matched for rostro-caudal plane, were captured using a Scanscope XT image scanner (Aperio Technologies, Vista, CA). Image J software was used to assist in quantification (Rasband, 1997-2014). For each section, both the area of the entire hippocampus and the area containing Thioflavin-S profiles were determined. These values were used to calculate an overall plaque burden per section (i.e., the total area of Thioflavin-S stained profiles/total hippocampal area X 100 = % of hippocampal area containing Thioflavin-S stained profiles). These estimates were averaged across sections to obtain an overall estimate of plaque burden for each animal (Chakrabarty et al., 2015). Comparisons of plaque burden between 3 and 6 mo. $APP_{swe}PS1$ mice were conducted using an unpaired t-test.

Western blotting procedures—Hippocampal expression of the presynaptic marker synaptophysin (SYN), the postsynaptic protein scaffold postsynaptic density-95 (PSD-95), and glial fibrillary acid protein (GFAP) was evaluated by Western blotting using homogenates prepared from behaviorally naïve 6 mo. $APP_{swe}PS1$ (n=7) and NTg (n=5) mice. Proteins were denatured and reduced in Laemmli sample buffer with 5% β-

mercaptoethanol (Fisher, Pittsburgh, PA, USA) and heated at 100° for 10 min. Twenty μg of protein per lane was electrophoretically separated on a Tris-glycine gel (4-15%) at 200 V for 35 min, and then transferred to Millipore Immobilon-FL PVDF membranes. Blots were washed 3 times with TBS (pH 7.4) then blocked for 1 h in TBS containing 5% milk and 0.01% Tween. The following antibodies were used: mouse monoclonal [SY38] to synaptophysin (ABCAM, 1:5,000 overnight incubation; (Chakrabarti et al., 2007; Konopka et al., 2010)), rabbit polyclonal to PSD-95 (ABCAM, 1:5,000; (Chakrabarti et al., 2007; Konopka et al., 2010)), chicken polyclonal antibody to GFAP (Encor, 1:2,000; (Bruijnzeel et al., 2011)), and a mouse monoclonal antibody to glyceraldehyde 3-phosphate dehydrogenase (GAPDH; EnCor, 1:10,000; (Fortun et al., 2003; Rangaraju et al., 2009)). All primary antibodies were incubated overnight at 4° with rotation and were detected using appropriate LI-COR IRDye secondary antibodies conjugated to 800CW (1:10,000). Secondary incubations were performed at room temperature for 1 h with rotation. Infrared signal was detected with the Odyssey Imager system (LI-COR) and measured with Image Studio software (LI-COR) as described previously (Kumar et al., 2015). Synaptophysin, PSD-95, and GFAP values were normalized to GAPDH measured in the same lanes to control for loading variation, and were expressed as a percentage of mean expression from NTg mice included on the same gel. Normalized values for each protein were compared between groups using unpaired t-tests.

Hippocampal Slice Preparation and Electrophysiological recordings—To evaluate synaptic function, electrophysiological recordings were performed in acute slices prepared from behaviorally naïve 6 mo. $APP_{swe}PS1$ (n=3) and NTg, littermate control mice (NTg; n=3). The methods for hippocampal slice preparation have been published previously (Brim et al., 2013; Kumar et al., 2015; Sharrow et al., 2002). Briefly, mice were anesthetized with halothane (Halocarbon Laboratories, River Edge, NJ), rapidly decapitated, hippocampi were dissected, and slices (~400 μm) through hippocampus were cut parallel to the alvear fibers using a tissue chopper (Technical Products International, St. Louis, MO). Slices (n=11 NTg, n=11 $APP_{swe}PS1$) were transferred to a standard interface-recording chamber that was continuously perfused (1 ml/min) with oxygenated artificial cerebrospinal fluid (aCSF) containing (in mM) 124 NaCl, 2 KCl, 1.25 KH_2PO_4, 2 $MgSO_4$, 2 $CaCl_2$, 26 $NaHCO_3$, and 10 glucose. Slices were maintained at 30 ± 0.5°, with humidified air (95% O_2-5% CO_2).

The methods for extracellular recordings from CA3-CA1 hippocampal slices obtained from mice have been previously published (Brim et al., 2013; Foster et al., 2008; Fugger et al., 2001; Kumar et al., 2015; Sharrow et al., 2002). Briefly, extracellular field excitatory postsynaptic potentials (fEPSP) were recorded with aCSF-filled glass micropipettes (4-6 MΩ). A recording electrode was placed in the stratum radiatum of the CA1 subfield. Two concentric bipolar stimulating electrodes (outer pole: stainless steel, 200 μm diameter; inner pole: platinum/iridium, 25 μm diameter, FHC, Bowdoinham, ME) were positioned approximately 1 mm on either side of the recording electrode. A single diphasic stimulus pulse of 100 μsec was delivered at 0.033 Hz to the Schaffer collateral commissural pathway using a stimulator (SD 9 Stimulator, Grass Instrument Co, West Warwick, RI), in order to evoke field potentials. The signals were sampled at 20 kHz, amplified, and filtered between 1 Hz and 1 kHz using Axoclamp-2A (Molecular Devices) and a differential AC amplifier

(A-M Systems). Field potential data were stored on a computer hard drive for off-line analysis. To measure the amplitude of the fEPSP, two cursors were placed to encompass the entire waveform. A SciWorks computer algorithm (Datawave Technologies) was used to compute the maximum amplitude (mV) at the peak of the waveform and to compute input-output curves for fEPSP. To determine whether any genotype differences in fEPSP could be attributable to differences in the number of stimulated fibers, the fiber potential amplitude (mV) was recorded across increasing stimulus intensities (V). To assess the paired-pulse ratio, pulse pairs were delivered through a single stimulating electrode at various interpulse intervals (50, 100, 200, and 300 ms). The first pulse was set to elicit 50% of the maximal fEPSP, as determined by the input–output curve. Five paired responses were recorded for each interpulse interval (note that one NTg slice was no longer viable at the time of this experiment). Finally, a subset of the slices (n=8 NTg, n=9 $APP_{swe}PS1$; slices came from all mice used in the other electrophysiological analyses) was used for evaluation of long-term potentiation (LTP). Synaptic responses were collected for at least ten minutes prior to pattern stimulation to ensure a stable baseline before induction of LTP. A high frequency pattern stimulation was used to induce LTP, which consisted of four 1 s trains of 100 Hz, with each train 10 seconds apart. The percent change from baseline in the fEPSP slope was used to evaluate changes in transmission properties induced by pattern stimulation. These values were compared from 10-60 min following LTP induction (after responses to test pulses had stabilized).

Two factor repeated-measures ANOVAs (genotype × stimulus intensity for total fEPSP and fiber potential, genotype × inter-pulse interval for paired-pulse facilitation, and genotype × time for LTP) were used to compare the effects of genotype on measures of synaptic function. Slices were used as the units of analysis.

Behavioral Testing and Data Analysis—A total of 25 mice at 3 and 6 months of age were used for behavioral testing in the transfer learning task ($APP_{swe}PS1$: 3 mo. (n=6) and 6 mo. (n=8); NTg: 3 mo. (n=5) and 6 mo. (n=6)). Testing in the transfer learning task was conducted as described above in Experiment 1. Performance on initial discrimination (trials to criterion) and transfer learning (percent error) was analyzed using two-factor ANOVA, with age and genotype as between-subjects factors. Odor detection threshold testing was analyzed using a three-factor repeated measures ANOVA (age × genotype × dilution), with dilution as the within-subjects factor.

Experiment 3: Transfer learning performance in the Dutch-Iowa model of amyloidosis

Subjects—Mice were generated by homozygous crossing of C57BL/6-Tg(Thy1-APPswDutIowa) BWevn/J (Davis et al., 2004). F1 pups were genotyped at 2 months of age, and female Tg-SwDI mice (as well as C57BL/6 mice used as NTg controls) were transferred to the AAALAC-accredited vivarium in the McKnight Brain Institute (University of Florida College of Medicine) where they were individually housed and allowed to habituate to vivarium conditions with *ad libitum* access to food and water for at least one month prior to the onset of behavioral experiments. Mice used in the transfer learning task were food-restricted to 85% of their free-feeding weight for one week prior to behavioral testing and

handled for 3-5 minutes daily to habituate to the experimenter. Upon completion of behavioral testing, mice were returned to *ad libitum* food.

Tissue Harvesting and Aβ Assessment—Using procedures identical to those described in Experiment 2, the hippocampi were harvested from a cohort of behaviorally naïve Tg-SwDI (n=6, 6 mo.) and C57BL/6 (n=3, 6 mo.) mice to assess Aβ40 and Aβ42 expression.

Behavioral Testing and Data Analysis—A total of 12 mice (6 mo.) were used for behavioral testing in the transfer learning task (n=6 Tg-SwDI and n=6 C57BL/6). Testing in the transfer learning task was conducted as described above in Experiments 1 and 2. Performance on initial discriminations (trials to criterion) and transfer learning (percent error) was analyzed using unpaired t-tests.

RESULTS

Experiment 1. Dependence of transfer generalization learning on hippocampus

Hippocampal Lesion Verification—Histological evaluation of sections from lesioned mice revealed loss of the pyramidal cell layers (CA1-CA3) throughout the entire rostro-caudal extent of the hippocampus. There was no evidence of damage to surrounding entorhinal cortex, and dorsal subiculum was largely intact, but some damage to ventral subiculum was observed in all mice (mean % damage = 45%, with a range of 20-70%). There was no evidence of damage in sham-lesioned mice. Figure 1A shows photomicrographs of representative sections from a sham and lesioned mouse, and Figure 1B shows a schematic reconstruction of the minimum and maximum extent of damage across the entire group. The hippocampal lesions were complete or nearly so in 7 of the 8 mice (90-100% damage), and hence these mice were included in subsequent analyses. One mouse had essentially no lesion-induced damage, and was excluded from further analyses.

Performance on the Transfer Learning Task—Sham- and hippocampal-lesioned mice did not differ in the number of trials required to reach criterion performance on the shaping discrimination problem prior to beginning the transfer learning task (Fig 1C, $t_{(13)} = 1.15$, $p = 0.27$). On the transfer learning task itself, the two groups also did not differ in their performance on the learning phase of the task (Fig 1D, Problem Set 1: $t_{(13)} = 1.48$, $p = 0.16$; Fig 1E, Problem Set 2: $t_{(13)} = 0.56$, $p = 0.59$). In contrast, the hippocampal-lesioned group made significantly more errors than the sham group on the transfer phase (Fig 1F, $t_{(13)} = 2.30$, $p = 0.04$), indicating an impaired ability to transfer the previously-learned associations to the new problem sets in which the stimulus features irrelevant to the correct choices were replaced with novel stimuli. Because the extent of damage to the ventral subiculum varied across subjects (see previous section), transfer learning performance was evaluated in relation to this damage. There were no correlations between the extent of damage to the ventral subiculum and any measure of performance on the transfer learning task ($rs < 0.28$, $ps > 0.54$).

Odor Detection Threshold—Odor detection threshold was assessed to determine whether the hippocampal lesions interfered with the ability of the mice to detect and respond

to the odorants. The two groups required similar numbers of trials to reach criterion on the initial discrimination between a full-strength odorant and mineral oil ($t_{(13)} = 0.64$, $p = 0.54$; Fig 2A). As expected, a two-factor repeated measures ANOVA revealed that the number of errors increased when the concentration of the full-strength odorant was diluted ($F_{(3,39)} = 5.28$, $p = 0.004$). Importantly, however, there was neither a main effect of lesion condition ($F_{(1,13)} = 0.60$, $p = 0.45$) nor an interaction between lesion condition and odorant dilution ($F_{(3,39)} = 0.67$, $p = 0.58$), indicating that the lesions did not interfere with the ability of the mice to detect and respond to odorants in the context of the discrimination task (Fig 2B).

Experiment 2: Synaptic dysfunction and transfer learning performance in the APPswePS1 model of amyloidosis

β-amyloid peptide accumulation—In agreement with previous studies, $APP_{swe}PS1$ mice showed age-dependent accumulation of Aβ40 and Aβ42 (Fig 3A). A one-factor ANOVA comparing Aβ levels in dissected hippocampi from NTg and $APP_{swe}PS1$ mice revealed significant group effects for both peptides (Aβ40: $F_{(2,13)}=8.91$, $p = 0.004$; Aβ42: $F_{(2,13)} = 5.84$, $p = 0.02$). Tukey HSD post-hoc tests revealed that levels of both Aβ40 and Aβ42 were higher in 6 mo. $APP_{swe}PS1$ mice compared to both 3 mo. $APP_{swe}PS1$ mice and NTg control mice (ps < 0.05 for both comparisons). Consistent with these findings, analysis of plaque area revealed a significant increase in thioflavin-positive profiles in 6 mo. compared to 3 mo. $APP_{swe}PS1$ mice (Fig 3B, $t_{(9)} = 2.48$, $p = 0.04$).

Measures of synaptic dysfunction—To provide an initial measure of synaptic integrity in 6 mo. $APP_{swe}PS1$ mice, expression of synaptophysin and PSD-95 was evaluated in homogenates prepared from dissected hippocampus using Western blotting (Fig 3C). Glial fibrillary acidic protein (GFAP) expression was evaluated in the same tissue, as an increase in astroglial markers has been observed in both pathological and normal aging (Barrientos et al., 2015; Ritzel et al., 2015a; Ritzel et al., 2015b; Simpson et al., 2010). Unpaired t-tests revealed that synaptophysin expression was significantly decreased in 6 mo. $APP_{swe}PS1$ compared to NTg mice (Fig 3D, $t_{(9)} = 2.96$, $p = 0.02$). In contrast, neither PSD-95 (Fig 3E, $t_{(9)} = 0.26$, $p = 0.81$) nor GFAP (Fig 3F, $t_{(9)} = 0.88$, $p = 0.40$) differed by genotype.

To further evaluate synaptic integrity, field potential recordings were performed at CA3-CA1 hippocampal synapses in 6 mo. $APP_{swe}PS1$ and age-matched non transgenic mice (n=11 slices from n=3 mice of each genotype). Input-output curves for total fEPSP were compared using a two-factor repeated measures ANOVA (genotype × stimulus intensity). This analysis indicated significant main effects of stimulus intensity ($F_{(11,220)} = 84.97$, $p = 0.001$), genotype ($F_{(1,20)} = 5.82$, $p = 0.03$) and an interaction between stimulus intensity and genotype ($F_{(11,220)} = 2.25$, $p = 0.01$). As shown in Fig 3G, while increasing voltage resulted in increased fEPSP amplitude across both $APP_{swe}PS1$ and NTg mice, this effect was attenuated in $APP_{swe}PS1$ mice, particularly at the highest stimulus intensities. These findings indicate that baseline synaptic transmission is reduced in 6 mo. $APP_{swe}PS1$ mice. In contrast, a similar analysis of fiber potential amplitude (Fig 3H) revealed a main effect of stimulus intensity ($F_{(11,220)} = 19.30$, $p = 0.01$) but neither a main effect of genotype ($F_{(1,20)} = 0.52$, $p = 0.48$) nor a genotype × stimulus intensity interaction ($F_{(11,220)} = 0.29$, $p = 0.99$). This analysis indicates that there are no differences in the numbers of axons stimulated in

$APP_{swe}PS1$ and NTg mice, showing that the reduction in synaptic transmission is not likely due to loss of afferent fibers. Paired-pulse facilitation, a form of presynaptic short-term plasticity, was also evaluated (Fig 3I). The analysis indicated a main effect of inter-pulse interval ($F_{(5,95)} = 165.23$, $p = 0.001$) but neither a main effect of genotype ($F_{(1,19)} = 2.98$, $p = 0.10$) nor a genotype × inter-pulse interval interaction ($F_{(5,95)} = 1.45$, $p = 0.21$). Finally, in order to investigate genotype effects on long-term synaptic plasticity, we recorded LTP at CA3-CA1 synapses in slices obtained from $APP_{swe}PS1$ and NTg mice. Analysis of LTP data (Fig 3J) revealed no main effect of genotype ($F_{(1,15)} = 1.69$, $p = 0.21$) but a main effect of time-point ($F_{(98,1470)} = 4.62$, $p = 0.001$) as well as a genotype × time-point interaction ($F_{(98,1470)} = 1.41$, $p = 0.007$), indicating that LTP decayed more rapidly in slices from $APP_{swe}PS1$ compared to NTg mice.

Assessment of hippocampal-dependent transfer learning—Transfer learning performance was assessed in 3 and 6 mo. $APP_{swe}PS1$ and age-matched NTg control mice using a between-subjects design, to determine the sensitivity of this aspect of hippocampal function to Aβ pathology and synaptic dysfunction. A two-factor ANOVA (age × genotype) revealed no differences between $APP_{swe}PS1$ and NTg mice on the shaping discrimination problem (Fig 4A, main effect of age: $F_{(1,21)} = 0.09$, $p = 0.76$; main effect of genotype: $F_{(1,21)} = 0.00$, $p = 0.99$; age × genotype interaction: $F_{(1,21)} = 0.01$, $p = 0.93$). Similarly, there were no differences during initial learning of the compound discrimination problems (Fig 4B, Problem Set 1: main effect of age: $F_{(1,21)} = 0.00$, $p = 0.97$; main effect of genotype: $F_{(1,21)} = 0.01$, $p = 0.92$; age × genotype interaction: $F_{(1,21)} = 0.49$, $p = 0.49$; Fig 4C, Problem Set 2: main effect of age: $F_{(1,21)} = 0.20$, $p = 0.53$; main effect of genotype: $F_{(1,21)} = 0.00$, $p = 0.96$; age × genotype interaction: $F_{(1,21)} = 0.18$, $p = 0.68$). In contrast, $APP_{swe}PS1$ mice showed significant impairments in transfer learning at 6 mo. compared to age-matched NTg controls (Fig 4D). A two-factor ANOVA (age × genotype) revealed no effect of genotype ($F_{(1,21)} = 1.33$, $p = 0.26$) but a significant main effect of age ($F_{(1,21)} = 21.05$, $p = 0.001$) as well as a significant interaction between age and genotype ($F_{(1,21)} = 5.21$, $p = 0.03$). Post-hoc comparisons between groups further revealed that 6 mo. $APP_{swe}PS1$ mice made significantly more errors than both 6 mo. NTg control and 3 mo. $APP_{swe}PS1$ mice ($ps < 0.05$).

Odor Detection Thresholds—Odor detection threshold was assessed to determine whether $APP_{swe}PS1$ genotype altered the ability to detect and respond to the odorants. A two-factor repeated measures ANOVA (age × genotype) revealed no differences between groups on the number of trials to reach criterion on the initial discrimination between a full-strength odorant and mineral oil (Fig 5A; main effect of age: $F_{(1,17)} = 4.30$, $p = 0.05$; main effect of genotype: $F_{(1,17)} = 0.65$, $p = 0.43$; age × genotype interaction: $F_{(1,17)} = 0.77$, $p = 0.39$). When the full-strength odorant was diluted at 1:100, 1:1000, and 1:10000, a three-factor repeated measures ANOVA (age × genotype × dilution) revealed a main effect of dilution ($F_{(2,34)} = 16.33$, $p = 0.001$) such that errors increased with lower odorant concentrations, a main effect of age ($F_{(1,17)} = 7.86$, $p = 0.01$) such that, across genotypes, 6 mo. mice performed worse than 3 mo. mice, but no main effect of genotype ($F_{(1,17)} = 1.65$, $p = 0.22$; Fig 5B). In addition, there were no interactions between age × dilution ($F_{(1,17)} = 0.62$, $p = 0.55$), genotype × dilution ($F_{(2,34)} = 2.04$, $p = 0.15$) or age × genotype × dilution

($F_{(2,34)}$ = 0.22, p = 0.80). There was a significant interaction between age × genotype ($F_{(1,17)}$ = 6.83, p = 0.02); however, this interaction was driven by the fact that 6 mo. NTg control mice made more errors than $APP_{swe}PS1$ mice, suggesting that impairments in olfactory function in $APP_{swe}PS1$ mice did not account for the transfer learning deficit evident at this age.

Experiment 3: Transfer learning performance in the Dutch-Iowa model of amyloidosis

Assessment of Aβ expression in the hippocampus of Tg-SwDI and non-transgenic control mice—In agreement with previous studies (Davis et al., 2004; Wilcock, 2004), 6 mo. Tg-SwDI mice showed significantly higher levels of Aβ40 and Aβ42 in the hippocampus compared to age-matched non-transgenic controls (Fig 6). Unpaired t-tests revealed that levels of both Aβ40 ($t_{(7)}$ = 6.33, p = 0.001) and Aβ42 ($t_{(7)}$ = 6.75, p = 0.001) were significantly higher in Tg-SwDI than in non-transgenic control mice..

Assessment of hippocampal-dependent transfer learning—Transfer learning performance was assessed in 6 mo. Tg-SwDI and age-matched NTg control (C57BL/6) mice, to determine whether the deficits observed in $APP_{swe}PS1$ mice in Experiment 2 were evident in a different mouse model of amyloidosis. Tg-SwDI and NTg control mice did not differ in the number of trials required to reach criterion performance on the shaping discrimination problem prior to beginning the transfer learning task (Fig 7A, $t_{(10)}$ = 1.66, p = 0.13). On the transfer learning task itself, the two groups also did not differ in their performance on the learning phase of the task (Fig 7B, Problem Set 1: $t_{(10)}$ = 0.95, p = 0.36; Fig 7C, Problem Set 2: $t_{(10)}$ = 1.44, p = 0.18). In contrast, Tg-SwDI mice made significantly more errors than NTg controls on the transfer phase (Fig 7D, $t_{(10)}$ = 3.89, p = 0.003), indicating an impaired ability to transfer the previously-learned stimulus-reward associations to the new problem sets.

As an additional analysis, performance on the transfer learning task was compared directly between the mice from Experiment 3 and the 6 mo. mice from Experiment 2. Performance of transgenic mice on the transfer phase was expressed as a percentage of their respective controls. This analysis revealed that the magnitude of impairment on the transfer phase in Tg-SwDI mice (276.6% of C57BL/6 controls) was significantly greater than that in $APP_{swe}PS1$ mice (145.2% of NTg controls) ($t_{(12)}$ = 3.52, p = 0.004). Although this difference should be interpreted with caution given that C57BL/6 controls performed better than NTg controls at 6 months of age (compare Figures 4D and 7D), it is consistent with the higher levels of Aβ expression in Tg-SwDI compared to $APP_{swe}PS1$ mice.

DISCUSSION

The mouse transfer learning task described herein was designed as a rodent analogue of a human task that is both sensitive to hippocampal damage and predictive of cognitive decline in aged individuals (Montgomery et al., 2011; Myers et al., 2002; Myers et al., 2008b). The goals of the current experiment were to determine if the mouse transfer learning task is dependent upon an intact hippocampus, and secondly, whether this task is sensitive to early synaptic changes in mouse models of amyloidosis. Although mice with hippocampal lesions were unimpaired in their ability to learn initial discriminations between olfactory or digging

media stimuli, the lesioned mice showed robust impairments in transferring this learning to novel stimulus configurations. Subsequent experiments characterized synaptic dysfunction in the hippocampus at relatively young ages (6 mo.) in the $APP_{swe}PS1$ mouse model of amyloidosis, and revealed concomitant impairments in transfer learning. Similar deficits were evident in a second mouse model of amyloidosis (Tg-SwDI), supporting the utility of assaying this aspect of hippocampal function as a sensitive detector of Aβ-mediated cognitive dysfunction. These findings significantly extend previous work demonstrating transfer learning deficits in older $APP_{swe}PS1$ mice (Montgomery et al., 2011) and forge stronger links with studies of transfer learning in humans (Myers C, 2003; Myers et al., 2002; Myers et al., 2008b). Together, these findings suggest that, across species, the ability to transfer learned information across contexts may be impaired by even subtle hippocampal pathology.

Hippocampus and transfer learning

The hippocampus is critical for the ability to apply learned information from a familiar context to a novel context or situation. Evidence that the hippocampus is involved in transfer learning finds empirical support in studies showing that individuals with hippocampal damage "unitize" stimuli during learning, resulting in impairments when aspects of the learned stimuli are altered (Barense et al., 2005; Quamme et al., 2007). Unitization refers to inflexible learning of compound stimuli as if they were one. For example, if "A" and "B" are different stimuli but are presented in combination such that "AB➔reward", unitization of these stimuli would result in learning that only the AB compound (as opposed to A and B individually) predicts reward. Eichenbaum and colleagues have shown that rats with lesions of the hippocampal formation display intact learning of AB➔reward associations, but display no evidence of this learning when interrogated about the nature of the A➔reward or B➔reward associations (Eichenbaum et al., 1988; Eichenbaum and Mathews, 1989). These findings indicate that learned information about the AB compound is "unitized", such that the individual stimuli within the compound are not represented independently, and thus cannot be transferred to novel situations in which A or B are presented alone. It is likely that the impairment on the transfer learning task in hippocampal lesioned mice in Experiment 1 represents a similar "unitization" phenomenon. Lesioned mice showed intact acquisition of the initial discrimination problems (Problem Sets 1 and 2), which consisted of compound stimuli composed of odors and digging media, but in which only one of these stimulus dimensions was relevant to detecting the food reward. In contrast, lesioned mice were impaired when required to use the information learned about the stimuli predictive of reward in a novel context (i.e., against the background of a novel odor or digging medium), despite the fact that the stimuli relevant for reward detection remained unchanged.

The hippocampal lesions in Experiment 1 were large, and encompassed the majority (90-100%) of the CA3, CA1, and dentate subregions. Consistent with the scope of the lesions, the magnitude of the transfer learning deficit was also large; however, unlike some tasks sensitive to hippocampus and medial temporal lobe damage [e.g., some forms of spatial and contextual learning (Kim and Fanselow, 1992; Morris et al., 1982)], the lesions did not abolish performance during the transfer phase of the task. Although it is conceivable that this reflects compensation by extra-hippocampal brain regions, it is more likely that the

ability of lesioned mice to perform the discriminations during the transfer phase at greater than chance accuracy reflects the fact that the transfer discriminations could still be acquired as if they were novel problems (i.e., without reference to the previous learning during Problem Sets 1 and 2).

Damage to the hippocampus and medial temporal lobe are reported to impair some forms of learning on olfactory-based tasks. For example, lesions of the CA2 subregion of the hippocampus impair social recognition memory in mice (Stevenson and Caldwell, 2014) and lesions of the dentate gyrus in rats attenuate performance at longer delays on an olfactory delayed match-to-sample task (Weeden et al., 2014). Importantly, however, in these studies and others that have assessed lesions of the entire hippocampus (Bunsey and Eichenbaum, 1995; Kaut and Bunsey, 2001), odor detection and discrimination remained intact, suggesting that hippocampal damage does not impair olfactory abilities *per se*. The transfer learning task used here requires detection and responses to olfactory cues, and hence mice were tested for olfactory acuity using decreasing concentrations of odorants. Lesioned mice showed odor detection thresholds comparable to controls, suggesting that lesion-induced olfactory deficits do not account for the impairment in transfer learning. Further, the absence of differences between odor detection threshold in lesioned and control mice is consistent with the intact performance of lesioned mice on the initial learning phase of the task (Problem Sets 1 and 2, in which half of the problems required olfactory discrimination learning). Considered together, these data support the hypothesis that hippocampal damage selectively impaired the ability to transfer previously-learned information to a novel context.

Transfer learning in APPswePS1 mice

$APP_{swe}PS1$ double-transgenic mice develop predictable and progressive age-related amyloid pathology, without concomitant neuronal loss. These mice express a chimeric mouse/human amyloid precursor protein (APP; Mo/HuAPP695swe) and the mutant human presenilin 1 (PS1-dE9), both of which are implicated in early-onset autosomal dominant forms of AD (Gordon et al., 2001; Jankowsky et al., 2004; Kamenetz, 2003). Previous findings demonstrate that learning and memory function, including transfer learning, is intact in 3 month old $APP_{swe}PS1$ mice, likely due to the fact that this age precedes marked elevations in β-amyloid levels, deposition of neuritic plaques, and consequent structural and signaling dysfunction in hippocampus (Gordon et al., 2001; Montgomery et al., 2011; Perez-Cruz et al., 2011). Indeed, at 12 months of age, by which time extensive hippocampal Aβ pathology and synaptic dysfunction is evident (Bell et al., 2006; Garcia-Alloza et al., 2006; Jankowsky et al., 2004), $APP_{swe}PS1$ mice demonstrate robust transfer learning deficits (Montgomery et al., 2011). Notably, the transfer learning deficits reported in our prior study were not associated with spatial learning deficits, suggesting that transfer learning represents a particularly sensitive measure of β-amyloid-induced hippocampal dysfunction. The present results support this interpretation by demonstrating that $APP_{swe}PS1$ mice exhibit poor transfer learning performance much earlier than previously described, with robust impairments evident as early as 6 months of age. Indeed, a growing literature suggests that Aβ-induced disruption of synaptic function contributes to cognitive deficits that can emerge in prodromal AD, well before the widespread neurodegeneration that is associated with later stages of the disease (Gruart et al., 2008; Jack et al., 2011; Jack et al., 2012; Masliah et al.,

1994). Although the extent of such synaptic dysfunction in mouse models of amyloidosis has been debated, the bulk of the evidence suggests that Aβ overproduction degrades synaptic integrity, particularly in the hippocampus (Buxbaum et al., 1998; Masliah et al., 1994; Sze et al., 2000; Wong, 1999). Findings from the present study are consistent with the view that synaptic function in hippocampus is compromised in 6 month old $APP_{swe}PS1$ mice. Immunoblotting revealed a modest but significant reduction in synaptophysin expression, and electrophysiological studies further demonstrated a decrement in excitatory transmission and plasticity at CA3-CA1 synapses. Specifically, these latter studies revealed a significant reduction in fEPSP amplitude in the hippocampus of 6 month old $APP_{swe}PS1$ relative to age-matched NTg mice. Moreover, the $APP_{swe}PS1$ mice show an accelerated decay of long-term potentiation, a model of the cellular substrates of memory storage. These findings provide strong evidence for the presence of synaptic impairments in the hippocampus of $APP_{swe}PS1$ mice by 6 months of age. As described in the current study, both Aβ40 and Aβ42 levels are significantly elevated by this age in $APP_{swe}PS1$ mice; however Aβ deposition in the hippocampus is not widespread (Burgess et al., 2006; Holcomb, 1998; Jankowsky et al., 2004; Wengenack et al., 2000). These data agree with a growing literature that suggests that soluble β amyloid can detrimentally impact neuronal communication and synaptic integrity, even in the absence of extensive plaque deposition (Jack et al., 2011; Jack et al., 2012; Oddo et al., 2003).

Consistent with the evidence for hippocampal synaptic dysfunction, 6 month old $APP_{swe}PS1$ mice were impaired on the transfer learning task relative to age-related NTg mice and 3 month old $APP_{swe}PS1$ mice. As in Experiment 1, these deficits were limited to the transfer phase of the task, suggestive of a specific impairment in the ability to transfer previously-learned information to a novel context rather than in procedural aspects of the task. The magnitude of this impairment was comparable to that observed following hippocampal lesions in Experiment 1, demonstrating that pronounced behavioral impairments in transfer learning do not require widespread hippocampal damage and are, instead, detectable even in the presence of modest hippocampal dysfunction. These data from mice agree with previous findings from Myers et al. (2002) in which aged but non-demented human subjects with mild hippocampal atrophy exhibited robust transfer learning deficits. Together, these studies suggest that the ability to transfer learned information across contexts may represent an aspect of hippocampal-mediated cognition that is particularly sensitive to amyloid pathology and synaptic dysfunction associated with aging and early stages of AD. It is important to note, however, that $APP_{swe}PS1$ mice present Aβ and plaque pathology in extrahippocampal brain regions as well, and thus that the present findings do not exclude potential contributions of dysfunction in other brain regions to the transfer learning deficits in these mice.

The transfer learning deficits reported at 6 months of age in the current study are among the earliest cognitive deficits described in $APP_{swe}PS1$ mice. Although there is one report of impaired radial arm water maze performance in 4 month old $APP_{swe}PS1$ mice (Park et al., 2006), reliable deficits in most hippocampus-dependent learning tasks (including contextual fear conditioning, Morris water maze, and Barnes maze) are typically not evident until well after 6 months of age (Cramer et al., 2012; Lalonde, 2004; Reiserer et al., 2007; Volianskis et al., 2010), with deficits across tasks becoming more reliable at quite advanced ages (i.e.,

>15 mo., (Webster et al., 2014)). The contrast between the robustness of the hippocampal-dependent transfer learning deficits by 6 months of age and the more subtle deficits observed in other hippocampal-mediated tasks at this age highlights the potential utility of transfer learning as a sensitive index of amyloid-induced hippocampal dysfunction. Within that context, it is notable that research in human subjects showed that transfer learning performance in non-demented elderly subjects predicted two year cognitive outcomes (normal, mild cognitive impairment, or probable AD) with a high degree of accuracy (Myers et al., 2008b).

Transfer learning deficits in Tg-SwDI mice

Current guidelines for conducting preclinical research in AD recommend the inclusion of multiple mouse models in order to ensure that results have broad applicability to a particular disease mechanism, rather than representing a unique phenotype of one particular model (Shineman et al., 2011). Accordingly, transfer learning was assessed in a second transgenic mouse model of amyloidosis. The Tg-SwDI mouse model is made with a construct containing the human amyloid beta-precursor protein, *APP* gene, with the Swedish K670N/M671L, Dutch E693Q, and Iowa D694N mutations (triple mutation) (Davis et al., 2004). Although this model has been characterized less extensively in comparison to the $APP_{swe}PS1$ model, Tg-SwDI mice exhibit more aggressive amyloid pathology (Davis et al., 2004; Kruyer et al., 2015; Miao et al., 2005; Xu et al., 2007). Indeed, in the current study, hippocampal levels of both Aβ40 and 42 even at 6 months of age were approximately 30 times greater in the Tg-SwDI mice compared to age-matched NTg controls. Consistent with this high level of Aβ production, Tg-SwDI mice showed robust transfer learning impairments compared to NTg mice. The impairment was selective to the transfer phase of the task, in that performance on the learning phase in Tg-SwDI mice did not differ from NTg controls. The magnitude of the impairment in Tg-SwDI mice appeared greater than in APPswePS1 mice; however, this magnitude difference may not necessarily relate to the level of amyloid pathology. It is notable that the NTg control mice in Experiment 3 performed particularly well on the transfer learning task, which may have contributed to the larger deficit observed in the Tg-SwDI mice. While synaptic function in Tg-SwDI mice has not been specifically examined, vascular amyloid deposition, which is prominent in Tg-SwDI, has been associated with attenuated synaptic plasticity in the hippocampus in other mouse models (Crouzin et al., 2013; Gouras et al., 2014; Hu et al., 2008; Pozueta et al., 2013; Steele et al., 2014; Thal et al., 2008). Although future work will be required to determine the mechanisms downstream of β-amyloid that mediate behavioral deficits in the Tg-SwDI model, the robust transfer learning impairments reported in the current study demonstrate that this aspect of hippocampal function is broadly sensitive to amyloid pathology.

Concluding Points

Previous work shows that assessments of transfer generalization learning can detect subtle deficits in hippocampal function in humans (Fera et al., 2014; Gluck et al., 2006; Myers C, 2003; Myers et al., 2002). The results described here demonstrate that performance in a formally identical task designed for use in mice (Montgomery et al., 2011) clearly depends upon an intact hippocampus. Importantly, however, performance on this task is also

sensitive to more subtle synaptic dysfunction resulting from Aβ deposition in two mouse models of amyloidosis. Findings described here demonstrate cognitive deficits at an earlier age than typically reported in the $APP_{swe}PS1$ model and show that these behavioral deficits are associated with β-amyloid induced synaptic dysfunction in the hippocampus. This enhanced sensitivity may offer advantages for early detection of cognitive decline. Moreover, the ability to assess transfer learning similarly across species could offer increased translational potential between preclinical animal models and clinical populations.

ACKNOWLEDGEMENTS

We thank Dr. Nicholas W. Simon (University of Pittsburg) for help with the ibotenic acid lesions, and Dr. Eduardo Candelario-Jalil (University of Florida) for assistance in optimizing the Western blot protocols. We also thank Dr. Todd Golde at the Center for Translational Research in Neurodegenerative Disease (University of Florida) for allowing us to use the Aperio equipment for the plaque counts, and Dr. Thomas C. Foster at the Evelyn F. McKnight Center for Research on Cognitive Aging and Memory (University of Florida), for sharing of materials for the electrophysiology studies of synaptic activity.

Grant Sponsors: McKnight Brain Research Foundation (JLB) NIH F31AG037286 (KSM)

REFERENCES

Barense MD, Bussey TJ, Lee AC, Rogers TT, Davies RR, Saksida LM, Murray EA, Graham KS. Functional specialization in the human medial temporal lobe. Journal Neuroscience. 2005; 25:10239–10246. [PubMed: 16267231]

Barrientos RM, Kitt MM, Watkins LR, Maier SF. Neuroinflammation in the normal aging hippocampus. Neuroscience. 2015 In press(0).

Bell KFS, Ducatenzeiler A, Ribeiro-da-Silva A, Duff K, Bennett DA, Cuello AC. The amyloid pathology progresses in a neurotransmitter-specific manner. Neurobiology of Aging. 2006; 27:1644–1657. [PubMed: 16271419]

Brim BL, Haskell R, Awedikian R, Ellinwood NM, Jin L, Kumar A, Foster TC, Magnusson K. Memory in aged mice is rescued by enhanced expression of the GluN2B subunit of the NMDA receptor. Behavioural Brain Research. 2013; 238:211–226. [PubMed: 23103326]

Bruijnzeel AW, Bauzo RM, Munikoti V, Rodrick GB, Yamada H, Fornal CA, Ormerod BK, Jacobs BL. Tobacco smoke diminishes neurogenesis and promotes gliogenesis in the dentate gyrus of adolescent rats. Brain Research. 2011; 1413:32–42. [PubMed: 21840504]

Bunsey M, Eichenbaum H. Selective damage to the hippocampal region blocks long-term retention of a natural and nonspatial stimulus-stimulus association. Hippocampus. 1995; 5(6):546–556. [PubMed: 8646281]

Burgess BL, McIsaac SA, Naus KE, Chan JY, Tansley GH, Yang J, Miao F, Ross CJ, van Eck M, Hayden MR. Elevated plasma triglyceride levels precede amyloid deposition in Alzheimer's disease mouse models with abundant A beta in plasma. Neurobiology of Disease. 2006; 24(1):114–127. others. [PubMed: 16899370]

Buxbaum JD, Thinakaran G, Koliatsos V, O'Callahan J, Slunt HH, Price DL, Sisodia SS. Alzheimer amyloid protein precursor in the rat hippocampus: transport and processing through the perforant path. Journal of Neuroscience. 1998; 18(23):9629–9637. [PubMed: 9822724]

Cahill L, Vazdarjanova A, Setlow B. The basolateral amygdala complex is involved with, but is not necessary for, rapid acquisition of Pavlovian “fear conditioning”. European Journal of Neuroscience. 2000; 12(8):3044–3050. [PubMed: 10971645]

Chakrabarti L, Galdzicki Z, Haydar TF. Defects in Embryonic Neurogenesis and Initial Synapse Formation in the Forebrain of the Ts65Dn Mouse Model of Down Syndrome. The Journal of Neuroscience. 2007; 27(43):11483–11495. [PubMed: 17959791]

Chakrabarty P, Li A, Ceballos-Diaz C, Eddy James A, Funk Cory C, Moore B, DiNunno N, Rosario Awilda M, Cruz Pedro E, Verbeeck C. IL-10 Alters immunoproteostasis in APP mice, increasing

plaque burden and worsening cognitive behavior. Neuron. 2015; 85(3):519–533. others. [PubMed: 25619653]

Cramer PE, Cirrito JR, Wesson DW, Lee CYD, Karlo JC, Zinn AE, Casali BT, Restivo JL, Goebel WD, James MJ. ApoE-Directed therapeutics rapidly clear β-Amyloid and reverse deficits in AD mouse models. Science. 2012; 335(6075):1503–1506. others. [PubMed: 22323736]

Crouzin N, Baranger K, Cavalier M, Marchalant Y, Cohen-Solal C, Roman FS, Khrestchatisky M, Rivera S, Féron F, Vignes M. Area-specific alterations of synaptic plasticity in the 5XFAD mouse model of Alzheimer's disease: dissociation between somatosensory cortex and hippocampus. PLoS ONE. 2013; 8(9):e74667. [PubMed: 24069328]

Davis J, Xu F, Deane R, Romanov G, Previti ML, Zeigler K, Zlokovic BV, Van Nostrand WE. Early-onset and robust cerebral microvascular accumulation of amyloid β-protein in transgenic mice expressing low levels of a vasculotropic Dutch/Iowa mutant form of amyloid β-protein precursor. J Biol Chem. 2004; 279:20296–20306. [PubMed: 14985348]

Desmedt A, Aline M, René G, Robert J. The effects of ibotenic hippocampal lesions on discriminative fear conditioning to context in mice: impairment or facilitation depending on the associative value of a phasic explicit cue. Eur J Neurosci. 2003; 17(9):1953–1963. [PubMed: 12752795]

Dubois B, Feldman HH, Jacova C, Dekosky ST, Barberger-Gateau P, Cummings J, Delacourte A, Galasko D, Gauthier S, Jicha G. Research criteria for the diagnosis of Alzheimer's disease: revising the NINCDS-ADRDA criteria. Lancet Neurology. 2007; 6:734–746. others. [PubMed: 17616482]

Eichenbaum H, Cohen Neal J. Can we reconcile the declarative memory and spatial navigation views on hippocampal function? Neuron. 2014; 83(4):764–770. [PubMed: 25144874]

Eichenbaum H, Fagan A, Mathews P, Cohen NJ. Hippocampal system dysfunction and odor discrimination learning in rats: impairment or facilitation depending on representational demands. Behavioral Neuroscience. 1988; 102(3):331–339. [PubMed: 3395444]

Eichenbaum H, Kuperstein M, Fagan A, Nagode J. Cue-sampling and goal-approach correlates of hippocampal unit activity in rats performing an odor-discrimination Task. Journal of Neuroscience. 1987; 7(3):716–732. [PubMed: 3559709]

Eichenbaum H, Mathews P. Further studies of hippocampal representation during odor discrimination learning. Behavioral Neuroscience. 1989; 103:1207–1216. [PubMed: 2610913]

Etchamendy N, Desmedt A, Cortes-Torrea C, Marighetto A, Jaffard R. Hippocampal lesions and discrimination performance of mice in the radial maze: sparing or impairment depending on the representational demands of the task. Hippocampus. 2003; 13:197–211. [PubMed: 12699328]

Fera F, Passamonti L, Herzallah MM, Myers CE, Veltri P, Morganti G, Quattrone A, Gluck MA. Hippocampal BOLD response during category learning predicts subsequent performance on transfer generalization. Human Brain Mapping. 2014; 35(7):3122–3131. [PubMed: 24142480]

Ferreira LK, Diniz BS, Forlenza OV, Busatto GF, Zanetti MV. Neurostructural predictors of Alzheimer's disease: A meta-analysis of VBM studies. Neurobiology of Aging. 2011; 32(10): 1733–1741. [PubMed: 20005012]

Fortun J, Dunn WA, Joy S, Li J, Notterpek L. Emerging Role for Autophagy in the Removal of Aggresomes in Schwann Cells. The Journal of Neuroscience. 2003; 23(33):10672–10680. [PubMed: 14627652]

Foster TC, Rani A, Kumar A, Cui L, Semple-Rowland SL. Viral vector–mediated delivery of estrogen receptor-α to the hippocampus improves spatial learning in estrogen receptor-α knockout mice. Molecular therapy : the journal of the American Society of Gene Therapy. 2008; 16(9):1587–1593. [PubMed: 18594506]

Franklin, KBJ.; Paxinos, G. The mouse brain in stereotaxic coordinates. Elsevier: 2008.

Fugger HN, Kumar A, Lubahn DB, Korach KS, Foster TC. Examination of estradiol effects on the rapid estradiol mediated increase in hippocampal synaptic transmission in estrogen receptor α knockout mice. Neuroscience Letters. 2001; 309(3):207–209. [PubMed: 11514077]

Garcia-Alloza M, Robbins EM, Zhang-Nunes SX, Purcell SM, Betensky RA, Raju S, Prada C, Greenberg SM, Bacskai BJ, Frosch MP. Characterization of amyloid deposition in the APPswe/PS1dE9 mouse model of Alzheimer disease. Neurobiology of Disease. 2006; 24(3):516–524. [PubMed: 17029828]

Gluck MA, Myers C. Hippocampal mediation of stimulus representation: A computational theory. Hippocampus. 1993; 3(4):491–516. [PubMed: 8269040]

Gluck MA, Myers CE. Representation and association in memory: A neurocomputational view of hippocampal function. Current Directions in Psychological Sciences. 1995; 4(1):23–29.

Gluck MA, Myers CE, Nicolle MM, Johnson S. Computational models of the hippocampal region: implications for prediction of risk for Alzheimer's disease in non-demented elderly. Current Alzheimer Research. 2006; 3(3):247–257. [PubMed: 16842102]

Gordon MN, King DL, Diamond DM, Jantzen PT, Boyett KV, Hope CE, Hatcher JM, DiCarlo G, Gottschall WP, Morgan D. Correlation between cognitive deficits and Abeta deposits in transgenic APP+PS1 mice. Neurobiology Aging. 2001; 22(3):377–385. others.

Gouras GK, Willén K, Faideau M. The inside-out amyloid hypothesis and synapse pathology in Alzheimer's disease. Neurodegenerative Diseases. 2014; 13(2-3):142–146. [PubMed: 24080821]

Gruart A, López-Ramos JC, Muñoz MD, Delgado-García JM. Aged wild-type and APP, PS1, and APP + PS1 mice present similar deficits in associative learning and synaptic plasticity independent of amyloid load. Neurobiology Disease. 2008; 30(3):439–450.

Holcomb L, Gordon MN, McGowan E, Yu X, Benkovic S, Jantzen P, Wright K, Saad I, Mueller R, Morgan D, Sanders S, Zehr C, O'Campo K, Hardy J, Prada CM, Eckman C, Younkin S, Hsiao K, Duff K. Accelerated Alzheimertype phenotype in transgenic mice carrying both mutant amyloid precursor protein and presenilin 1 transgenes. Nature. 1998; 4:97–100.

Hu N-W, Smith IM, Walsh DM, Rowan MJ. Soluble amyloid-β peptides potently disrupt hippocampal synaptic plasticity in the absence of cerebrovascular dysfunction in vivo. 2008:2414–2424.

Jack C, Vemuri P, Wiste HJ. Evidence for ordering of alzheimer disease biomarkers. Archives of Neurology. 2011; 68(12):1526–1535. [PubMed: 21825215]

Jack, Cr; Vemuri, P.; Wiste, HJ., et al. Shapes of the trajectories of 5 major biomarkers of alzheimer disease. Archives of Neurology. 2012:1–12.

Jankowsky JL, Fadale DJ, Anderson J, Xu GM, Gonzales V, Jenkins NA, Copeland NG, Lee MK, Younkin LH, Wagner SL. Mutant presenilins specifically elevate the levels of the 42 residue β-amyloid peptide in vivo: evidence for augmentation of a 42-specific γ secretase. Human Molecular Genetics. 2004; 13(2):159–170. others. [PubMed: 14645205]

Jankowsky JL, Xu G, Fromholt D, Gonzales V, Borchelt DR. Environmental enrichment exacerbates amyloid plaque formation in a transgenic mouse model of Alzheimer disease. Journal of Neuropathology and Experimental Neurology. 2003; 62(12):1220–7. [PubMed: 14692698]

Johnson SC, Schmitz TW, Asthana S, Gluck MA, Myers CE. Associative learning over trials activates the hippocampus in healthy elderly but not mild cognitive impairment. Neuropsychology, Development and Cognition. Section B, Aging, Neuropsychology and Cogniton. 2008; 15:129–145.

Kamenetz F, Tomita T, Hsieh H, Seabrook G, Borchelt D, Iwatsubo T, Sisodia S, Malinow R. APP processing and synaptic function. Neuron. 2003; 37:925–937. [PubMed: 12670422]

Kaut KP, Bunsey MD. The effects of lesions to the rat hippocampus or rhinal cortex on olfactory and spatial memory: retrograde and anterograde findings. Cognitive, affective & behavioral neuroscience. 2001; 1(3):270–86.

Kesner RP, Hunsaker MR, Ziegler W. The role of the dorsal and ventral hippocampus in olfactory working memory. Neurobiology of Learning and Memory. 2011; 96(2):361–366. [PubMed: 21742047]

Kim JJ, Fanselow MS. Modality-specific retrograde amnesia of fear. Science. 1992; 256(5057):675–677. [PubMed: 1585183]

Kluger A, Ferris SH, Golomb J, Mittelman MS, Reisberg B. Neuropsychological prediction of decline to dementia in nondemented elderly. Journal of Geriatric Psychiatry and Neurology. 1999; 12(168-179)

Konopka W, Kiryk A, Novak M, Herwerth M, Parkitna JR, Wawrzyniak M, Kowarsch A, Michaluk P, Dzwonek J, Arnsperger T. MicroRNA Loss Enhances Learning and Memory in Mice. The Journal of Neuroscience. 2010; 30(44):14835–14842. others. [PubMed: 21048142]

Krishna R, Moustafa AA, Eby A, Skeen LC, CE M. Learning and generalization in healthy aging: implication for frontostriatal and hippocampal function. Cognitive and Behavioral Neurology. 2012; 25(1):7–15. [PubMed: 22353726]

Kruyer A, Soplop N, Strickland S, Norris EH. Chronic hypertension leads to neurodegeneration in the TgSwDI mouse model of Alzheimer's disease. Hypertension. 2015

Kumar A, Bean LA, Rani A, Jackson T, Foster TC. Contribution of estrogen receptor subtypes, ERα, ERβ, and GPER1 in rapid estradiol-mediated enhancement of hippocampal synaptic transmission in mice. Hippocampus. 2015 epub ahead of print.

Lalonde R, Kim HD, Fukuchi K. Exploratory activity, anxiety, and motor coordination in bigenic APPswe + PS1/DeltaE9 mice. Neuroscience Letters. 2004; 369(2):156–61. [PubMed: 15450687]

Lazarov O, Robinson J, Tang Y-P, Hairston IS, Korade-Mirnics Z, Lee VMY, Hersh LB, Sapolsky RM, Mirnics K, Sisodia SS. Environmental enrichment reduces Aβ levels and amyloid deposition in transgenic mice. Cell. 2005; 120(5):701–713. [PubMed: 15766532]

Levites Y, Das P, Price RW, Rochette MJ, Kostura LA, McGowan EM, Murphy MP, Golde TE. Anti-Aβ42– and anti-Aβ40–specific mAbs attenuate amyloid deposition in an Alzheimer disease mouse model. The Journal of Clinical Investigation. 2006a; 116(1):193–201. [PubMed: 16341263]

Levites Y, Smithson LA, Price RW, Dakin RS, Yuan B, Sierks MR, Kim J, McGowan E, Reed DK, Rosenberry TL. Insights into the mechanisms of action of anti-Aß antibodies in Alzheimer's disease mouse models. The FASEB Journal. 2006b; 20(14):2576–2578. others. [PubMed: 17068112]

Lowndes GJ, Saling MM, Ames D, Chiu E, Gonzalez LM, Savage GR. Recall and recognition of verbal paired associates in early Alzheimer's disease. Journal of the International Neuropsychological Society. 2008; 14(4):591–600. [PubMed: 18577288]

Mainardi M, Di Garbo A, Caleo M, Berardi N, Sale A, Maffei L. Environmental enrichment strengthens corticocortical interactions and reduces amyloid-β oligomers in aged mice. Frontiers in Aging Neuroscience. Jan.2014 6

Maruff P, Collie A, Darby D, Weaver-Cargin J, Masters C, Currie J. Subtle memory decline over 12 months in mild cognitive impairment. Dementia and Geriatric Cognitive Disorders. 2004; 18:342–348. [PubMed: 15316183]

Masliah E, Honer W, Mallory M, Voigt M, Kushner P, Hansen L, Terry R. Topographical distribution of synaptic-associated proteins in the neuritic plaques of Alzheimer's disease hippocampus. Acta Neuropathologica. 1994; 87(2):135–142. [PubMed: 8171963]

McKenzie S, Frank Andrea J, Kinsky Nathaniel R, Porter B, Rivière Pamela D, Eichenbaum H. Hippocampal representation of related and opposing memories develop within distinct, hierarchically organized neural schemas. Neuron. 2014; 83(1):202–215. [PubMed: 24910078]

Miao J, Xu F, Davis J, Otte-Höller I, Verbeek MM, Van Nostrand WE. Cerebral microvascular amyloid β protein deposition induces vascular degeneration and neuroinflammation in transgenic mice expressing human vasculotropic mutant amyloid β precursor protein. The American Journal of Pathology. 2005; 167(2):505–515. [PubMed: 16049335]

Montarolo F, Parolisi R, Hoxha E, Boda E, Tempia F. Early enriched environment exposure protects spatial memory and accelerates amyloid plaque formation in APPSwe/PS1L166P mice. PLoS ONE. 2013; 8(7)

Montgomery KS, Simmons RK, Edwards Iii G, Nicolle MM, Gluck MA, Myers CE, Bizon JL. Novel age-dependent learning deficits in a mouse model of Alzheimer's disease: Implications for translational research. Neurobiology of Aging. 2011; 32(7):1273–85. [PubMed: 19720431]

Moodley K, Minati L, Contarino V, Prioni S, Wood R, Cooper R, D'Incerti L, Tagliavini F, Chan D. Diagnostic differentiation of mild cognitive impairment due to Alzheimer's disease using a hippocampus-dependent test of spatial memory. Hippocampus. 2015 n/a-n/a.

Morris RG, Garrud P, Rawlins JN, O'Keefe J. Place navigation impaired in rats with hippocampal lesions. Nature. 1982; 297(5868):681–683. [PubMed: 7088155]

Myers C SD, Gluck M, Grossman S, Kluger A, Ferris S, Golomb J, Schnirman G, Schwartz R. Dissociating hippocampal versus basal ganglia contributions to learning and transfer. Journal of Cognitive Neuroscience. 2003; 15(2):185–193. [PubMed: 12676056]

Myers CE, Gluck MA. Cortico-hippocampal representations in simultaneous odor discrimination: a computational interpretation of Eichenbaum, Mathews, and Cohen (1989). Behavioral Neuroscience. 1996; 110:685–706. [PubMed: 8864261]

Myers CE, Hopkins R, DeLuca J, Moore N, Wolansky LJ, Sumner J, Guck M. Learning and generalization deficits in patients with memory impairments due to anterior communicating artery aneurysm rupture or hypoxic brain injury. Neuropsychology. 2008a; 22(5):681–686. [PubMed: 18763887]

Myers CE, Kluger A, Golomb J, Ferris SH, de Leon MJ, Schnirman G, Gluck MA. Hippocampal atrophy disrupts transfer generalization in nondemented elderly. Journal of Geriatric Psychiatry and Neurology. 2002; 15:82–90. [PubMed: 12083598]

Myers CE, Kluger A, Golomb J, Gluck MA, Ferris S. Learning and generalization tasks predict short-term cognitive outcome in nondemented elderly. Journal of Geriatric Psychiatry and Neurology. 2008b; 21(2):93–104. [PubMed: 18474718]

Oddo S, Caccamo A, Shepherd JD, Murphy MP, Golde TE, Kayed R, Metherate R, Mattson MP, Akbari Y, LaFerla FM. Triple-transgenic model of Alzheimer's disease with plaques and tangles: intracellular A beta and synaptic dysfunction. Neuron. 2003; 39(3):409–421. [PubMed: 12895417]

Park JH, Widi GA, Gimbel DA, Harel NY, Lee DHS, Strittmatter SM. Subcutaneous Nogo receptor removes brain amyloid-β and improves spatial memory in Alzheimer's transgenic mice. The Journal of Neuroscience. 2006; 26(51):13279–13286. [PubMed: 17182778]

Perez-Cruz C, Nolte MW, van Gaalen MM, Rustay NR, Termont A, Tanghe A, Kirchhoff F, Ebert U. Reduced spine density in specific regions of CA1 pyramidal neurons in two transgenic mouse models of Alzheimer's disease. The Journal of Neuroscience. 2011; 31(10):3926–3934. [PubMed: 21389247]

Pozueta J, Lefort R, Shelanski ML. Synaptic changes in Alzheimer’s disease and its models. Neuroscience. 2013; 251(0):51–65. [PubMed: 22687952]

Quamme JR, Yonelinas AP, Norman KA. Effect of unitization on associative recognition in amnesia. Hippocampus. 2007; 17:192–200. [PubMed: 17203466]

Rabin LA, Wang C, Katz MJ, Derby CA, Buschke H, Lipton RB. Predicting Alzheimer's disease: neuropsychological tests, self-reports, and informant reports of cognitive difficulties. Journal of the American Geriatrics Society. 2012; 60(6):1128–34. [PubMed: 22690986]

Rangaraju S, Hankins D, Madorsky I, Madorsky E, Lee W-H, Carter CS, Leeuwenburgh C, Notterpek L. Molecular architecture of myelinated peripheral nerves is supported by calorie restriction with aging. Aging Cell. 2009; 8(2):178–191. [PubMed: 19239416]

Rasband, WS. ImageJ, U. S. National Institutes of Health; Bethesda, Maryland, USA: 1997-2014. http://imagej.nih.gov/ij/

Reiserer RS, Harrison FE, Syverud DC, McDonald MP. Impaired spatial learning in the APPSwe + PSEN1DeltaE9 bigenic mouse model of Alzheimer's disease. Genes, Brain and Behavior. 2007; 6(1):54–65.

Ritzel RM, Patel AR, Pan S, Crapser J, Hammond M, Jellison E, McCullough LD. Age- and location-related changes in microglial function. Neurobiology of Aging. 2015a Epub ahead of print(0).

Ritzel RM, Patel AR, Pan S, Crapser J, Hammond M, Jellison E, McCullough LD. Age- and location-related changes in microglial function. Neurobiology of Aging. 2015b In press(0).

Rudy JW, Sutherland RJ. Configural association theory and the hippocampal formation: An appraisal and reconfiguration. Hippocampus. 1995; 5(5):375–389. [PubMed: 8773252]

Sharrow KM, Kumar A, Foster TC. Calcineurin as a potential contributor in estradiol regulation of hippocampal synaptic function. Neuroscience. 2002; 113(1):89–97. [PubMed: 12123687]

Shineman D, Basi G, Bizon J, Colton C, Greenberg B, Hollister B, Lincecum J, Leblanc G, Lee L, Luo F. Accelerating drug discovery for Alzheimer's disease: best practices for preclinical animal studies. Alzheimer's Research & Therapy. 2011; 3(5):28. others.

Silva D, Guerreiro M, Maroco J, Santana I, Rodrigues A, Marques JB, de Mendonça A. Comparison of four verbal memory tests for the diagnosis and predictive value of mild cognitive impairment. Dementia and Geriatric Cognitive Disorders Extra. 2012; 2(1):120–131. [PubMed: 22590473]

Simpson JE, Ince PG, Lace G, Forster G, Shaw PJ, Matthews F, Savva G, Brayne C, Wharton SB. Astrocyte phenotype in relation to Alzheimer-type pathology in the ageing brain. Neurobiology of Aging. 2010; 31(4):578–90. [PubMed: 18586353]

Stargardt A, Swaab DF, Bossers K. The storm before the quiet: Neuronal hyperactivity and Aβ in the presymptomatic stages of Alzheimer's disease. Neurobiology of Aging. 2015; 36(1):1–11. [PubMed: 25444609]

Steele JW, Brautigam H, Short JA, Sowa A, Shi M, Yadav A, Weaver CM, Westaway D, Fraser PE, St George-Hyslop PH. Early fear memory defects are associated with altered synaptic plasticity and molecular architecture in the TgCRND8 Alzheimer's disease mouse model. Journal of Comparative Neurology. 2014; 522(10):2319–2335. others. [PubMed: 24415002]

Stevenson EL, Caldwell HK. Lesions to the CA2 region of the hippocampus impair social memory in mice. European Journal of Neuroscience. 2014; 40(9):3294–3301. [PubMed: 25131412]

Sze C-I, Bi H, Kleinschmidt-DeMasters BK, Filley CM, Martin LJ. Selective regional loss of exocytotic presynaptic vesicle proteins in Alzheimer's disease brains. Journal of the Neurological Sciences. 2000; 175(2):81–90. [PubMed: 10831767]

Thal DR, Griffin WST, Braak H. Parenchymal and vascular Aβ-deposition and its effects on the degeneration of neurons and cognition in Alzheimer's disease. Journal of Cellular and Molecular Medicine. 2008; 12(5b):1848–1862. [PubMed: 18624777]

Thompson M, Knee K, Golden C. Olfaction in persons with Alzheimer's disease. Neuropsychology Review. 1998; 8(1):11–23. [PubMed: 9585920]

Velayudhan L, Gasper A, Pritchard M, Baillon S, Messer C, P P. Pattern of Smell Identification Impairment in Alzheimer's Disease. Journal of Alzheimer's Disease. 2015 Epub ahead of print.

Volianskis A, Køstner R, Mølgaard M, Hass S, Jensen MS. Episodic memory deficits are not related to altered glutamatergic synaptic transmission and plasticity in the CA1 hippocampus of the APPswe/PS1ΔE9-deleted transgenic mice model of β-amyloidosis. Neurobiology of Aging. 2010; 31(7):1173–1187. [PubMed: 18790549]

Webster SJ, Bachstetter AD, Nelson PT, Schmitt FA, Van Eldik LJ. Using mice to model Alzheimer's dementia: an overview of the clinical disease and the preclinical behavioral changes in ten mouse models. Frontiers in Genetics. 2014:5. [PubMed: 24523726]

Weeden CSS, Hu NJ, Ho LUN, Kesner RP. The role of the ventral dentate gyrus in olfactory pattern separation. Hippocampus. 2014; 24(5):553–559. [PubMed: 24449260]

Wengenack TM, Whelan S, Curran GL, Duff KE, Poduslo JF. Quantitative histological analysis of amyloid deposition in Alzheimer's double transgenic mouse brain. Neuroscience. 2000; 101(4):939–944. [PubMed: 11113343]

Wilcock DM, Rojiani A, Rosenthal A, Subbarao S, Freeman MJ, Gordon MN, Gordon D. Passive immunotherapy against Abeta in aged APP-transgenic mice reverses cognitive deficits and depletes parenchymal amyloid deposits in spite of increased vascular amyloid and microhemorrhage. Journal of Neuroinflammation. 2004; 1:24. [PubMed: 15588287]

Wong TP, Debeir T, Duff K, Cuello AC. Reorganization of cholinergic terminals in the cerebral cortex and hippocampus in transgenic mice carrying mutated presenilin-1 and amyloid precursor protein transgenes. Journal of Neuroscience. 1999; 19:2706–2716. [PubMed: 10087083]

Xu F, Grande AM, Robinson JK, Previti ML, Vasek M, Davis J, Van Nostrand WE. Early-onset subicular microvascular amyloid and neuroinflammation correlate with behavioral deficits in vasculotropic mutant amyloid β-protein precursor transgenic mice. Neuroscience. 2007; 146(1):98–107. [PubMed: 17331655]

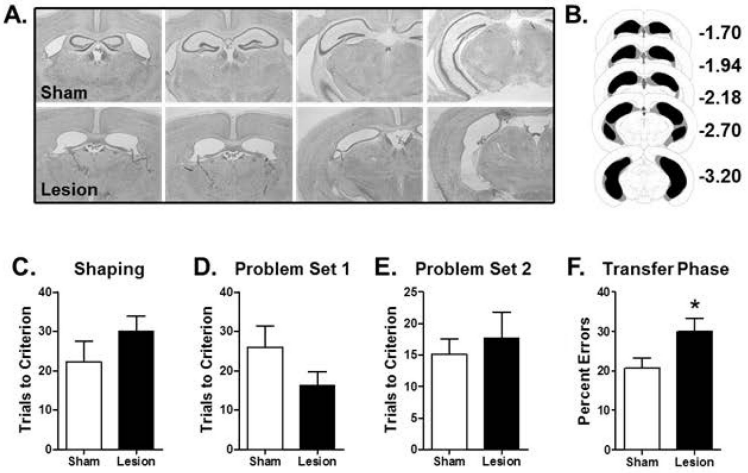

Figure 1. Effects of hippocampal lesions on transfer learning

(A) Photomicrographs of Nissl-stained sections through the hippocampus of a representative sham (top) and lesioned (bottom) mouse. (B) Schematic shows the minimum (black) and maximum (gray) extent of the hippocampal lesions across all mice. (C) Bar graph shows mean number of trials (+SEM) required to reach criterion performance on the shaping problem prior to testing in the transfer learning task. (D) Bar graph shows mean number of trials (+SEM) to reach criterion on Problem Set 1 of the learning phase of the transfer task. (E) Bar graph shows mean number of trials (+SEM) to reach criterion on Problem Set 2 of the learning phase of the transfer task. (F) Bar graph shows mean percentage of incorrect choices (errors +SEM) on the transfer phase of the task. Lesioned mice made significantly more errors than sham control mice. See text for statistical analysis. * $p < 0.05$ compared to sham group.

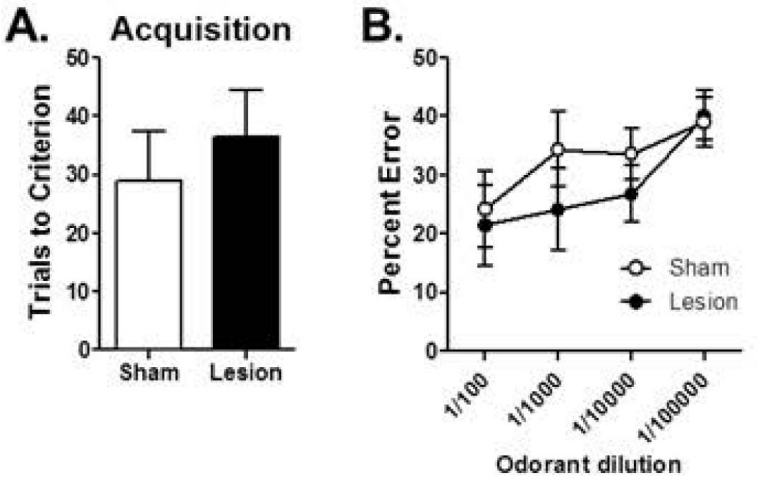

Figure 2. Effects of hippocampal lesions on odor detection threshold

(A) Bar graph shows mean number of trials (+SEM) required to reach criterion performance on a novel odor discrimination problem (full strength). (B) Line graph shows mean (±SEM) percentage of errors on the same odor discrimination problem as in (A) but with serial dilutions of the target odorant. Sham control and lesioned mice performed similarly across the range of odorant dilutions.

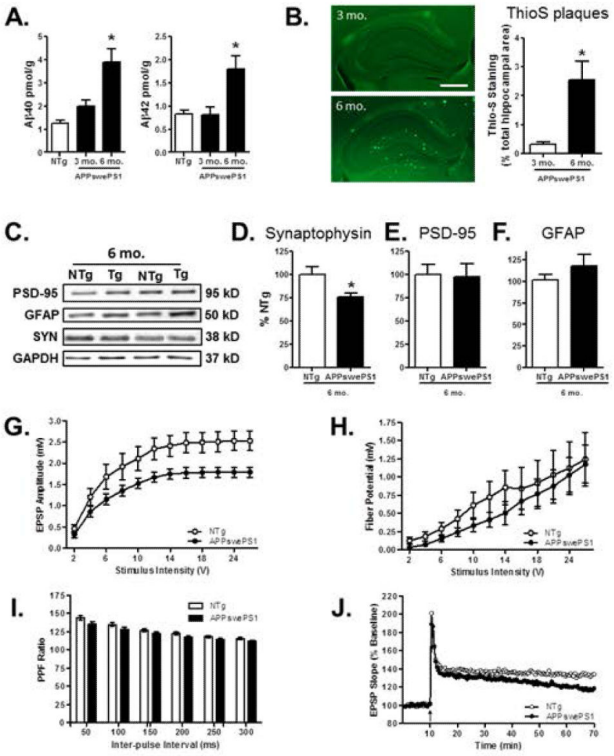

Figure 3. Amyloid and synaptic measures in the hippocampus of APP_{swe} PS1 and NTg control mice

(A) Bar graphs show mean (+SEM) levels of Aβ40 and Aβ42 peptides in the hippocampus of 6 mo. NTg control and 3 and 6 mo. APP_{swe}PS1 mice. Both Aβ40 and Aβ42 were significantly increased in 6 mo. APP_{swe}PS1 mice compared to 3 mo. APP_{swe}PS1 and NTg mice. (B) Photomicrographs showing thioflavin-S staining for amyloid plaques (bright green puncta) in the hippocampus of representative 3 and 6 mo. APP_{swe}PS1 mice. Scale bar = 500 μm. Plaque area (Thio-S staining as a percentage of total hippocampal area) was significantly greater in 6 than 3 mo. APP_{swe}PS1 mice. (C) Representative immunoreactive bands detected in hippocampal homogenates prepared from 6 mo. NTg and APP_{swe}PS1 (Tg) mice following incubation with antibodies to synaptophysin, PSD-95, GFAP, and the loading control GAPDH. (D-F) Bar graphs show mean (+SEM) hippocampal expression of each protein, expressed as a percentage of NTg mice processed on the same gel. Synaptophysin expression (D) was significantly reduced in APP_{swe}PS1 compared to NTg mice. In contrast, neither PSD-95 (E) nor GFAP (F) expression differed between APP_{swe}PS1 and NTg mice. (G) Line graph shows mean fEPSP (±SEM) amplitude at CA3-CA1 synapses in 6 mo. NTg and APPswePS1 mice, plotted as a function of stimulus intensity. The fEPSP amplitude was significantly reduced in APP_{swe}PS1 compared to NTg mice. (H) Line graph shows mean fiber potential amplitude (±SEM) at CA3-CA1 synapses in NTg and APPswePS1 mice, plotted as a function of stimulus intensity. (I) Bar graph shows mean paired-pulse facilitation ratio (+SEM) at CA3-CA1 synapses in NTg and APP_{swe}PS1 mice, plotted as a function of inter-pulse interval. (J) Line graph shows the slope of fEPSPs in response to test pulses before and after tetanus (arrow) at CA3-CA1 synapses in NTg and APP_{swe}PS1 mice, expressed as a percentage of pre-tetanus baseline. The rate of

decay was significantly greater in $APP_{swe}PS1$ compared to NTg mice. See text for statistical analyses. * $p < 0.05$ compared to NTg and/or 3 mo. group.

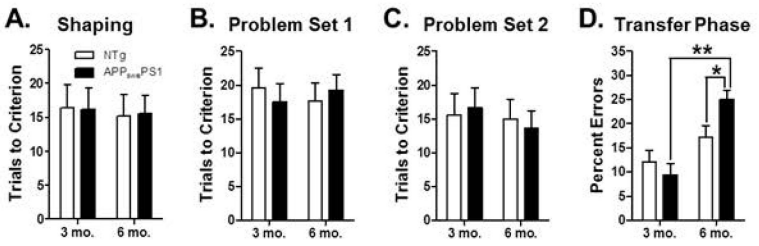

Figure 4. Hippocampal-dependent transfer learning performance in 3 and 6 month old $APP_{swe}PS1$ and NTg control mice

(A) Bar graph shows that mean number of trials (+SEM) required to reach criterion performance on the shaping problem prior to testing in the transfer learning task did not differ by age or genotype. (B & C) Bar graphs show that mean number of trials to reach criterion (+SEM) on Problem Set 1 (B) and Problem Set 2 (C) in the learning phase of the transfer task did not differ by age or genotype. (D) In contrast, 6 mo. but not 3 mo. $APP_{swe}PS1$ mice made significantly more incorrect choices (errors +SEM) on the transfer phase of the task relative to their respective age-matched NTg controls. In addition, 6 mo. $APP_{swe}PS1$ mice made significantly more errors than 3 mo. $APP_{swe}PS1$ mice. See text for statistical analysis. * $p < 0.05$, ** $p < 0.01$.

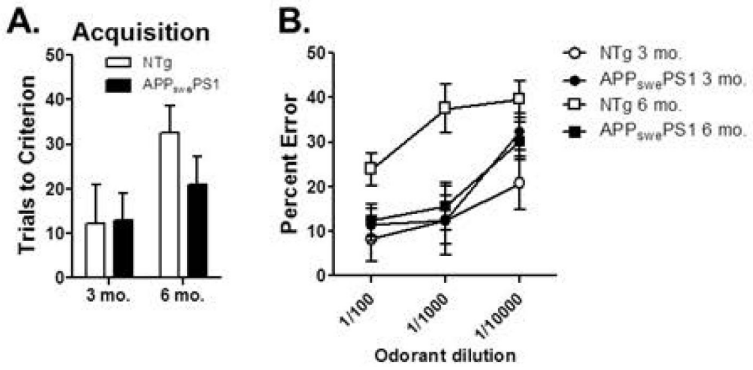

Figure 5. Odor detection threshold in APPswePS1 and NTg mice

(A) Bar graph shows mean number of trials (+SEM) required to reach criterion performance on a novel odor discrimination problem (full strength). (B) Line graph shows mean (±SEM) percentage of errors on the same odor discrimination problem as in (A) but with serial dilutions of the target odorant. Although 6 mo. mice as a group performed worse than 3 mo. mice, this effect was driven by worse performance in NTg compared to $APP_{swe}PS1$ mice at this age.

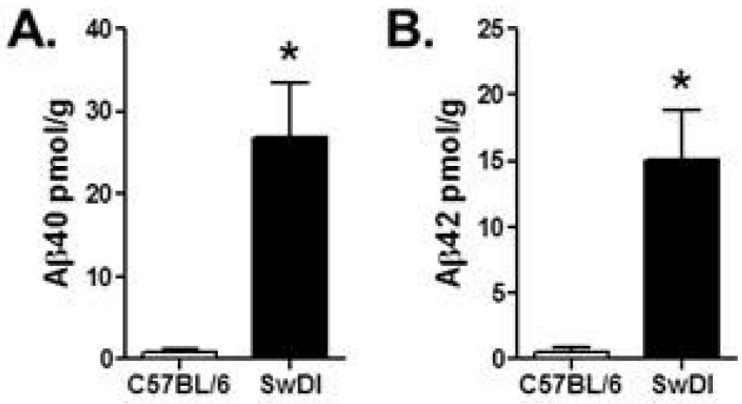

Figure 6. Amyloid measures in the hippocampus of Tg-SwDI and C57BL/6 control mice

Bar graphs show mean (+SEM) levels of Aβ40 (A) and Aβ42 (B) peptides in the hippocampus of 6 mo. C57BL/6 and Tg-SwDI mice. Expression of both Aβ40 and Aβ42 were significantly greater in Tg-SwDI mice compared to C57BL/6 mice.

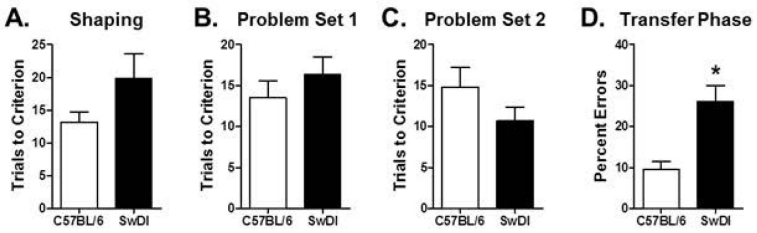

Figure 7. Hippocampal-dependent transfer learning performance in 6 month old Tg-SwDI and NTg control mice (C57BL/6)

(A) Bar graph shows mean (+SEM) number of trials required to reach criterion performance on the shaping problem prior to testing in the transfer learning task. (B) Bar graph shows mean (+SEM) number of trials to reach criterion on Problem Set 1 of the learning phase of the transfer task. (C) Bar graph shows mean (+SEM) number of trials to reach criterion on Problem Set 2 of the learning phase of the transfer task. (D) Bar graph shows mean (+SEM) percentage of incorrect choices (errors) on the transfer phase of the task. Tg-SwDI mice made significantly more errors than C57BL/6 (NTg) control mice. See text for statistical analysis. * $p < 0.05$ compared to C57BL/6 control group.